Title
Warm irrigation fluid effect on Thulium fiber laser (TFL) ablation of uroliths

Journal
Lasers in Medical Science, 40(1)

ISSN
0268-8921

Authors
Cumpanas, Andrei D
Katta, Nitesh
Vu, Thao N
et al.

Publication Date
2025

DOI
10.1007/s10103-024-04253-2

Lasers in Medical Science (2025) 40:112
https://doi.org/10.1007/s10103-024-04253-2

RESEARCH

Warm irrigation fluid effect on Thulium fiber laser (TFL) ablation of uroliths

Andrei D. Cumpanas[1] · Nitesh Katta[2] · Thao N. Vu[1] · Yi Xi Wu[1] · Antonio R. H. Gorgen[1] · Mariah C. Hernandez[1] · Kelvin Vo[1] · Sohrab N. Ali[1] · Zachary E. Tano[1] · Pengbo Jiang[1] · Roshan M. Patel[1] · Thomas Milner[2] · Jaime Landman[1] · Ralph V. Clayman[1]

Received: 25 September 2024 / Accepted: 5 December 2024

Abstract

Prior laser studies have demonstrated that as the temperature of a medium increases, the amount of energy delivered to the target increases. We sought to investigate the role of irrigation fluid temperature on Thulium fiber laser (TFL) urolith ablation. 360 calculi were divided in vitro according to chemical composition: calcium oxalate monohydrate (COM), cystine (CYS), struvite (STR), calcium phosphate (CAP), uric acid (UA), and calcium oxalate dihydrate (COD). A 200 µm TFL was placed directly on each stone, while immersed in 0.9% NaCl at four different temperatures (25 C, 37 C, 44 C, 60 C) and a single laser pulse administered at distinct energy settings (0.1 J, 0.5 J, 1.5 J). Optical coherence tomography assessed the resulting ablation cone volume. Mean stone volume and porosity were evaluated through ANOVA and Tukey post-hoc analysis. A multivariate generalized model for each composition accounted for the impact of fluid temperature and laser energy on stone ablation. Warmer fluid temperatures yielded greater ablation cone volumes for most energy settings, excluding UA stones. When accounting for chemical composition, higher tensile strength stones (COM, CYS) benefited most from warmer fluid in comparison to frangible stones (CAP, STR). The effects of increasing fluid temperature are modest relative to laser pulse energy as a large temperature increase (i.e. 7ºC) is equivalent to a minor energy increase (i.e. 0.1 J). For non-UA stones, TFL ablation efficiency increases with warmer irrigation fluid. The effect, albeit modest compared to laser pulse energy, was most notable for COM and CYS stones.

Keywords Nephrolithiasis · Thulium laser · Stone ablation · Irrigation fluid temperature · Stone composition · Laser lithotripsy

✉ Andrei D. Cumpanas
acumpana@hs.uci.edu

✉ Nitesh Katta
nkatta@uci.edu

✉ Thomas Milner
milnert@uci.edu

Thao N. Vu
thaonv@hs.uci.edu

Yi Xi Wu
yxwu@hs.uci.edu

Antonio R. H. Gorgen
gorgena@hs.uci.edu

Mariah C. Hernandez
mariahch@hs.uci.edu

Kelvin Vo
kelvinbv@hs.uci.edu

Sohrab N. Ali
sohrabna@hs.uci.edu

Zachary E. Tano
ztano@hs.uci.edu

Pengbo Jiang
pengboj@hs.uci.edu

Roshan M. Patel
roshanmp@hs.uci.edu

Jaime Landman
landmanj@hs.uci.edu

Ralph V. Clayman
rclayman@hs.uci.edu

[1] University of California, Irvine, Irvine, USA

[2] Beckman Laser Institute and Medical Clinic, Irvine, USA

Published online: 21 February 2025

Introduction

Since its first application in 2005, Thulium fiber laser lithotripsy has been the subject of numerous studies investigating its effectiveness in kidney stone therapy [1]. Despite its frequent clinical use, the precise physical mechanism behind Thulium laser lithotripsy and the optimal conditions for its use are still being elucidated.

The mechanism behind Thulium laser stone ablation has been primarily reported to be photothermal, with the laser beam-stone matrix interaction resulting in confined temperature increase both at the stone surface and within the stone itself [2, 3]. Researchers reasoned that temperature contributed to denaturation, stone softening, and eventually stone decomposition [4–8]. In addition to the photothermal phenomenon, other electron microscopy studies have shown stone cracking with minimal changes in stone composition after laser lithotripsy, thus questioning whether the stone ablation is solely the result of a photothermal effect [9]. Recently, it has been postulated that the rising water temperature within the cracks and pores of the stone plays a larger role [3–5]. In the photomechanical theory, the increase in temperature of the water inside the stone itself leads to rapid vapor expansion, formation of a vapor bubble, and thus stone fragmentation through explosive vaporization. Neither effect excludes the other, as *Taratkin et al.*. recently showed, and indeed both may well be operational. In their study, the photothermal chemical decomposition effect appeared to be more predominant in the earlier stages of laser lithotripsy, and the photomechanical effect was more predominant in the later stages of the lithotripsy [2].

The absorption coefficient is a measurement of the energy lost into the medium through which the laser beam is passing. *Jansen et al.*. were the first investigators to describe the effect that temperature changes have on the absorption coefficient of water for the midinfrared laser [10]. He found that an increase in water temperature decreased the absorption coefficient. As such, with higher temperatures of fluid irrigation, there would be less energy lost into the medium the beam is traversing, and thus more energy would be available to hit the stone's surface.

Accordingly, we sought to assess whether elevations in irrigation fluid temperature might result in increased stone ablation efficiency when employing the Thulium fiber laser to fragment uroliths of varying chemical compositions.

Materials and methods

Stone preparation

Three-hundred and sixty stones measuring 5–10 mm were separated into six groups of 60 stones each, based on their chemical composition: 100% calcium oxalate monohydrate (COM), 70–100% calcium oxalate dihydrate (COD), 100% calcium phosphate (CAP), 100% cystine (CYS), 100% struvite, and 100% uric acid (UA). In order to employ optical coherence tomography (OCT) to accurately assess the dimensions of the ablation cone created by the single discharge of the laser fiber, the superior and the anterior surface of each stone had to be planar. To achieve the necessary flat surfaces of the stones, we sanded each stone with 3 M Pro Grade Precision™ 60 Grit Coarse sanding paper. Next, each stone fragment was fixed on its inferior flat surface onto a glass plate using Loctite® Super Glue Gel; stones were placed at an equal distance from one another on the slide, such that each slide would accommodate five stones with a flat surface exposed (Fig. 1-A).

As there are no "dry" renal calculi in vivo, prior to the experiment, the stones were soaked in water at room temperature for 26 days. Soaking the stones removed a potential confounder, especially since any fluid within the stone likely plays a role in laser stone ablation [11].

Experimental set-up

A 36.98 × 26.97 × 17.98-inch glass tank was filled with 0.9% saline to create a water bath for the stone slides and mimic the irrigation fluid that would be used clinically during ureteroscopic Thulium laser stone ablation. A high-speed camera (HotShot 1280 INT, NAC Image Technology) with a frame rate of 20,000 fps was placed in front of the glass tank to capture the exact moment of stone ablation. A flexible digital ureteroscope (Flex X^C, Karl Storz™, Tuttlingen, Germany) was fixed above the water tank in a flexed position so that the tip of the Thulium laser fiber, when passed through the working channel of the flexible ureteroscope, would be perpendicular to the planar surface of the stone, as assessed by the high-speed camera images (Fig. 1-B).

Subsequently, each stone plate was independently submerged and placed onto a fixed platform within the tank, allowing the superior planar side of the stone to face the high-speed camera lens. The water temperature was manipulated using an electronic immersion water heater, while a thermometer probe was used to continuously monitor the irrigation fluid temperature throughout the experiment. For each group, stone ablation was completed at four different temperatures: 20 °C (room temperature), 37 °C (body temperature), 44 °C (urothelial thermal injury threshold),

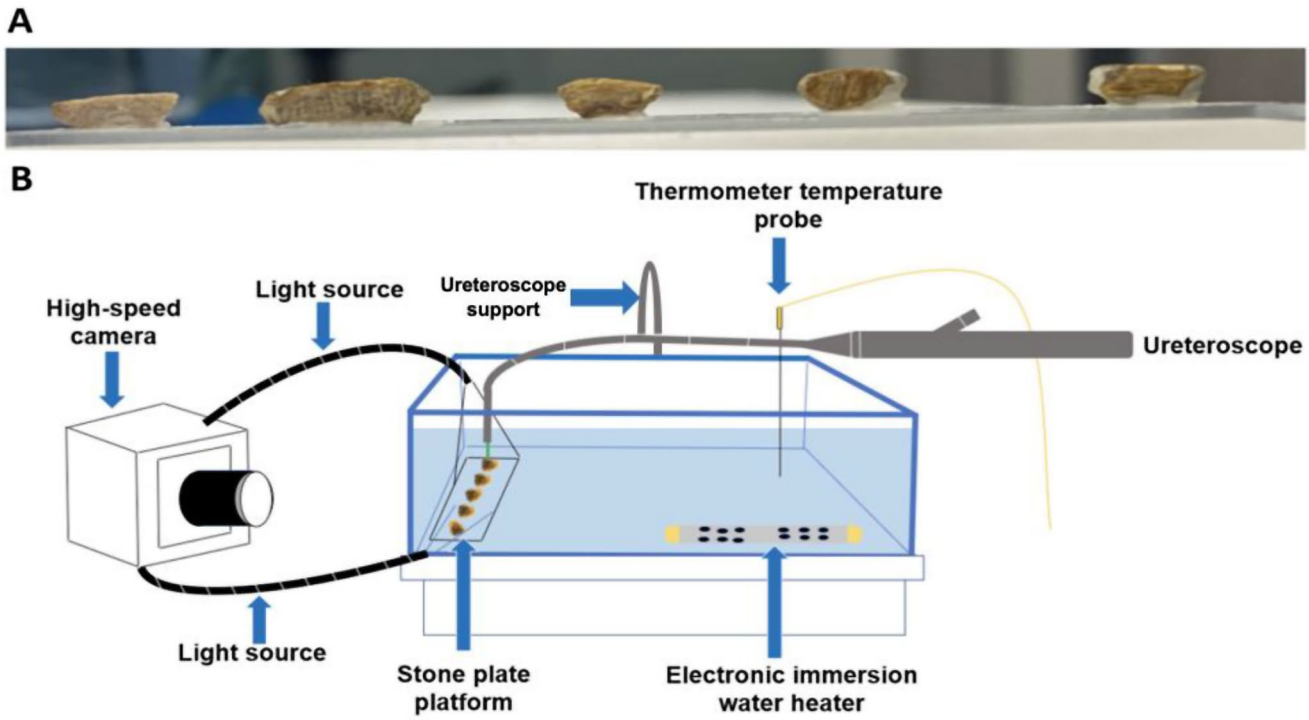

Fig. 1 Stone surface preparation (**A**) and experimental set-up (**B**)

and 60 °C (temperature used to ablate nerves crossing the renal pelvis to ameliorate essential hypertension) (Fig. 1-B). If the water tank temperature deviated by more than 2 °C from the set threshold, the experiment was paused to allow for a return to the targeted temperature. Once the irrigant temperature reached the desired threshold and stayed at that level consistently for 2–3 min, the experimental assessment was begun.

Laser settings

A 200 µm Thulium fiber laser (IPG Photonics, Boston, USA) was placed in direct contact with the surface of the stone. A single laser pulse with 100% peak power and at three different energy settings was directly applied to the set of stones irrigated at the same temperature: (1) 0.1 J and 200µs pulse duration; (2) 0.5 J and 1 ms pulse duration or (3) 1.5 J and 3 ms pulse duration. Typically, diode pumped fiber lasers (such as the Thulium fiber laser) are limited in peak power, unlike clinical flash-lamp pumped Holmium: YAG lasers. Therefore, in order to achieve the energy range tested (0.1 to 1.5 J), we extended the pulses while keeping the peak power constant at 100%, resulting in a corresponding 500 W. Each stone received a single laser pulse. We were aware that for single laser pulse application, the optimal methodology is to deliver the first ten pulses into a laser beam and then deliver the 10th or even 11th pulse to the target. This approach ensured that the Holmium laser is consistently delivering the specified pulse energy. This is not the case for the Thulium laser. Indeed, we assessed the laser energy emitted by the Thulium fiber laser across six series of 11 different laser shots and found no statistically significant energy difference between the 1st and $10^{th,}$ or 11th pulse in each series (Supplemental Table 1).

Post-ablation optical coherence tomography (OCT)

Optical coherence tomography (OCT), a non-destructive imaging technique, was used to generate a detailed surface image of each stone following a laser pulse allowing for precise measurement of the volume of the ablation cone generated by each laser pulse; the OCT level of resolution is approximately 10 µm, within a field of view of approximately 10×10 mm at a potential penetration depth of 1–2 mm. This is a non-invasive method of measurement that precludes any additional stone preparation [12, 13].

High-speed camera imaging assessment and ImageJ post-processing

Image J, an NIH-developed open-source software for image visualization and analysis was utilized for post-processing. The 360 high-speed camera videos were subsequently analyzed by a reviewer to ensure that (1) the sTFL tip was in contact with each stone, (2) the laser fiber tip was perfectly perpendicular to the stone surface and (3) the laser was fired

only once per stone. Out of the 360 runs, eight high-speed videos did not fit these criteria and were excluded from the analysis.

Statistical analysis

The ablation cone volume across different temperatures and energy settings was evaluated using two-tailed analysis of variance (ANOVA) testing followed by Tukey post hoc analysis in order to determine statistically significant results.

To assess the impact of changes in fluid temperature versus different energy levels on TFL stone ablation, we constructed a multivariate generalized linear model (MVGLM) for all chemical compositions (Fig. 2). β (beta weight) is a statistical metric used in MVGLMs that measures the relationship between a one-unit increase in the independent variables (i.e., temperature and energy) and the corresponding response in the dependent variable (i.e., the volume of the ablation cone). In our case, the β value enabled us to compare the stone ablation effect of a 1ºC increase in fluid temperature with a 0.1 J increase in laser energy, for each set of uroliths of different chemical compositions.

Results

When adjusting for irrigation fluid temperature, for all chemical compositions, an increase in pulse energy trended towards a statistically significant increase in ablation cone volume (Table 1; Fig. 2).

To assess the impact that changes in fluid temperature versus different energy levels had on sTFL stone ablation, we ran a MVGLM for all stone types. Stone composition, laser firing energy, and irrigation fluid temperature were all found to have a significant impact on stone ablation (Table 2). Notably, only for UA nephrolithiasis, was the fluid temperature not a significant factor in stone ablation efficiency at any energy setting. We found that for the same ablation laser energy applied to the stone surface, under similar irrigation temperature settings, STR and CYS stones had the highest and lowest ablation cone volumes, respectively.

Moreover, the MVGLM revealed that, on average, the increase in ablation efficiency when increasing the energy level by 0.1 J was equivalent to a 9ºC increase in fluid temperature (Table 2).

Fig. 2 Ablation cone volume (mm3) per single laser pulse using different energy settings and different irrigation fluid temperatures. The p-values were calculated by Tukey ANOVA post-hoc analysis. Symbol legend: * meaning $p<0.05$; ** meaning $p<0.01$; *** meaning $p<0.001$. The "ns" symbol indicates a non-significant difference

Discussion

Prior laser studies have demonstrated that a significant proportion (91–96%) of the laser energy is dissipated as heat into the surrounding irrigation [14]. As such, concerns regarding thermal-induced urothelial injuries from the heated irrigant are valid, especially since the damage may be irreversible and not immediately evident to the urologist during the lithotripsy procedure [15]. In this regard, it is important to note that irreversible thermal damage to biological tissues is not solely dependent on temperature but is also influenced by the duration of exposure itself [15, 16]. For instance, protein denaturation, cell necrosis, and apoptosis occur after 240 min of exposure to a temperature of the collecting system of 43ºC, while significantly shorter durations of only 28.1 and 7.1 s are sufficient for urothelial damage when calyceal temperature peaks at 51ºC and 53ºC [16, 17]. Moreover, given the recurrent nature of urolithiasis, with patients often requiring multiple surgeries over their lifetime, there is a potential risk of cumulative damage. This can, in time, result in scarring leading to ureteral or infundibular obstruction, with irreversible loss of renal function [15].

An adequate irrigation flow, the use of a ureteral access sheath (UAS), and intermittent laser activation have been proven to mitigate the risk of thermal-induced urothelial damage [16, 17]. Without irrigation, even 5 W of laser power for as short as 30 s causes thermal injury [17]. As such, at power settings of ≤20 W and ≥40 W, at least 15 and 40 mL/min of irrigation flow, respectively, are needed to maintain the collecting system temperature within the safe range [17]. *Okhunov et al.*. showed that the incidence of exceeding 44°C can be lessened by utilizing a UAS. Still, as pointed out by *Noureldin et al.*, even the use of a UAS can only compensate so much, with the detrimental temperature buffering effect waning when using higher laser power settings (40–60 W) [18, 19]. There's also evidence that intermittent laser activation (5 s on– 5 s off) can maintain the collecting system and ureteral temperatures within the safe thermal range [16, 20, 21]. This is important as during Thulium laser lithotripsy the stone itself acts as a "heat sink continuing to release thermal energy even when the laser is not firing. *Morgan et al.* showed that it would take 83 seconds to reach the urothelial damage threshold of 44°C when performing laser lithotripsy in the ureter with a 200µm TFL fiber at a "dusting" setting of 0.5 J, 80 Hz [20]. Of note, once the stone has been "heated" by continuous laser firing, even

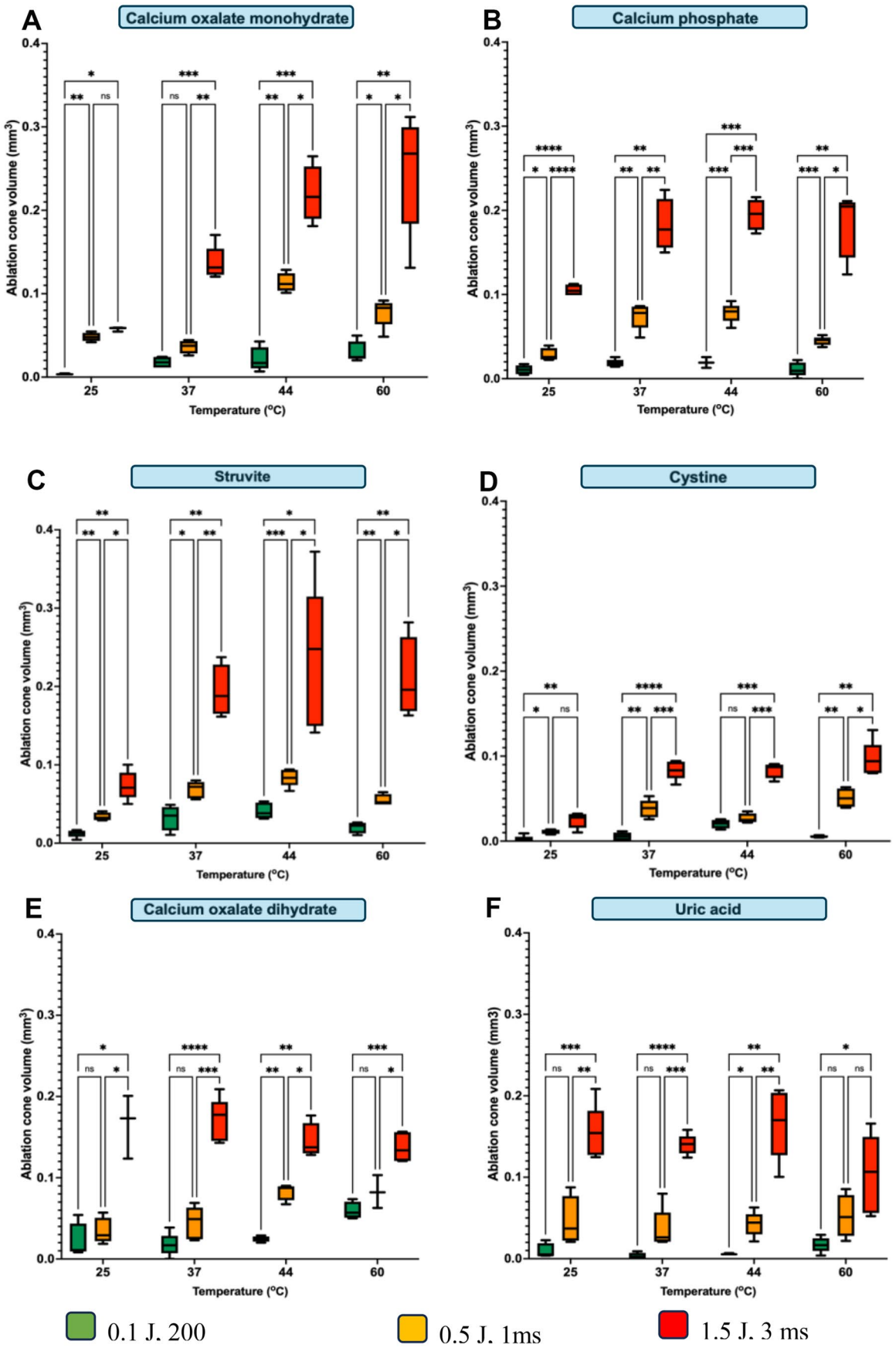
A
Calcium oxalate monohydrate
B
Calcium phosphate
C
Struvite
D
Cystine
E
Calcium oxalate dihydrate
F
Uric acid
Ablation cone volume (mm³)
Ablation cone volume (mm3)
Temperature (°C)
25
37
44
60
0.1 J. 200
0.5 J. 1ms
1.5 J. 3 ms

pausing lasering for 5 seconds does not bring the collecting system temperature back to baseline [20]. Indeed, under these circumstances, upon reactivating the laser, it only takes 5 seconds of continuous firing to reach 44ºC again [20]. Similarly, *Goldsmith et al.* noted that in 83% of cases, the temperature within the calyceal system was significantly higher ($p<0.01$) if the laser energy was delivered when a stone was present [22]. With the tip of a thermocouple in the very center of a BegoStone, *Marom et al.* showed that stone core temperatures increased after each cycle of laser activation and did not return to baseline between cycles [23]. Of note, temperatures as high as 120ºC were recorded within the core of the BegoStone [23].

In our study, except for uric acid stones, fluid temperature did indeed play a significant role in the ablation of urinary calculi; however, the effect was modest in comparison to that of a minimal increase in laser pulse energy. Indeed, albeit statistically significant, the effect of fluid temperature on stone ablation is not clinically relevant. Accordingly, the ablative advantage of using irrigation fluid set at 37 °C instead of room temperature (25 °C) irrigation fluid would be entirely neutralized by increasing the laser firing energy by 0.18 J. Also, our findings are specific to a single laser pulse applied to the stone surface. Moreover, the benefit of an augmented ablation cone volume at higher temperature (e.g. 44ºC), in the clinical environment of continuous laser firing for even 5 s "on" and 5 s "off" is greatly outweighed by the risk of urothelial cytotoxicity, especially since the stone serves as its own "heat sink" once it has been heated up by continuous laser firing for a minute or more [20]. Indeed, for ureteral stones, we currently use the 5 s "on" and 5 s "off" regimen throughout the procedure to avoid any excessive heat build-up and possible thermal induced, ureteral injury.

While chilled irrigation fluid might seem like a natural alternative due to its potential to lower thermal dose and better prevent thermal injury, its benefits are overshadowed by the significant risks of hypothermia and a higher incidence of postoperative fever and shivering [24, 25]. In contrast, using warmed irrigation (i.e., body temperature) has been shown to decrease postoperative complications and reduce associated pain [25, 26]. Accordingly, based on the current literature and the findings in our study, we recommend that the irrigation during thulium laser lithotripsy be set at 37ºC.

In light of significant concerns surrounding thermal-induced urothelial damage, appropriately fine-tuning laser parameters to maximize ablation volumes while lowering the cost of heat waste in the collecting system seems achievable by defining the appropriate laser ablation parameters for the different chemical stone compositions. Unfortunately, at this time, there is still a notable absence of standardized laser dosimetry protocols, leading to substantial variations among different healthcare institutions and even within the same institution. This is mainly due to the fact that while we can effectively address the medical condition at hand, we are far from fully comprehending the true mechanism behind laser lithotripsy's success and how this varies dependent upon the stone's composition. Of note, our data with the Thulium laser are in agreement with the Ho: YAG findings of *Sea et al.*, with the crater volume widening as the pulse energy of the laser increases [27].

Interestingly, although the same pulse energy was applied to all the different urolith chemical compositions, the volume of the resulting stone ablation cone varied markedly. Clearly, other factors, such as threshold radiant exposure, absorption coefficients, stone porosity, chemical bonds, and the tensile strength of the different chemical compositions play a role; the importance of each requires further study.

While *Chan et al.* evaluated the threshold radiant exposure (i.e., the minimum laser energy required to produce visual damage to the calculus surface) at 2.1 μm, to the best of our knowledge, no study to date evaluated this threshold at 1.9 μm, corresponding to the TFL emission wavelength [28]. Our data seem to suggest that the lowest threshold radiant exposure is seen for STR and the highest value for CYS.

In relation to the non-uric acid renal calculi crystal matrix deposition, water molecules can either be adsorbed to the crystal's surface or included within the matrix itself [29]. Interestingly, as shown by *Robinson et al.*, stones of different chemical compositions display different absorption patterns, with all water-containing kidney stones, except for struvite, absorbing laser energy more strongly at wavelengths associated with the Thulium fiber laser (1.94 μm) than with the Holmium: YAG (Ho: YAG) laser (2.12 μm) [29]. For STR stones, which are the uroliths with the highest water content, it seems the strong hydrogen bonds cause a transition of their absorption peak from higher to lower energies [29]. This would explain our findings, suggesting a lower threshold radiant exposure for STR stones. On the opposite end, CYS stones are less porous, and have a substantial number of disulfide bonds, which exhibit remarkable chemical strength and exceptional thermostability, consequently demanding higher energy levels for the disruption of the bonds within the stone's matrix [30]. Further studies are needed in this regard.

There are several limitations to our study. The first limitation is that we only evaluated the ablation effect of a single laser pulse on stones. While applying a single laser pulse to the stone's surface provides valuable insights into the laser-stone interaction, it does not replicate the complexities of a clinical scenario in which the laser is fired at varying frequencies and for a varying amount of time. Another limitation is the inclusion of high temperatures up to 60 °C, which

Table 1 The average volume ablated per single laser pulse. The average ablation volume was calculated for each fluid temperature for each stone type and energy setting level. The p-values were calculated through ANOVA tests; an asterisk (*) indicates statistical significance

		Mean 1	Mean 2	Mean difference	SE difference	*p*-value
COM	**25 °C**					
	Low energy vs. Medium energy	0.003600	0.04815	-0.04455	0.003180	0.0092*
	Low energy vs. High energy	0.003600	0.05760	-0.05400	0.001643	0.0243*
	Medium energy vs. High energy	0.04815	0.05760	-0.009450	0.005181	0.4636
	37 °C					
	Low energy vs. Medium energy	0.01778	0.03640	-0.01863	0.008564	0.2782
	Low energy vs. High energy	0.01778	0.1370	-0.1192	0.005989	0.0006*
	Medium energy vs. High energy	0.03640	0.1370	-0.1006	0.01152	0.0065*
	44 °C					
	Low energy vs. Medium energy	0.02190	0.1133	-0.09135	0.006234	0.0015*
	Low energy vs. High energy	0.02190	0.2201	-0.1982	0.01108	0.0001*
	Medium energy vs. High energy	0.1133	0.2201	-0.1069	0.01721	0.0171*
	60 °C					
	Low energy vs. Medium energy	0.03072	0.07742	-0.04670	0.01268	0.0451*
	Low energy vs. High energy	0.03072	0.2470	-0.2163	0.03059	0.0047*
	Medium energy vs. High energy	0.07742	0.2470	-0.1696	0.03524	0.0186*
CAP	**25 °C**					
	Low energy vs. Medium energy	0.01048	0.02828	-0.01780	0.004515	0.0230*
	Low energy vs. High energy	0.01048	0.1052	-0.09470	0.004241	<0.0001*
	Medium energy vs. High energy	0.02828	0.1052	-0.07690	0.005187	<0.0001*
	37 °C					
	Low energy vs. Medium energy	0.01838	0.07414	-0.05576	0.007077	0.0016*
	Low energy vs. High energy	0.01838	0.1822	-0.1638	0.01566	0.0034*
	Medium energy vs. High energy	0.07414	0.1822	-0.1081	0.01695	0.0061*
	44 °C					
	Low energy vs. Medium energy	0.01910	0.07812	-0.05902	0.006299	0.0002*
	Low energy vs. High energy	0.01910	0.1950	-0.1759	0.009874	0.0002*
	Medium energy vs. High energy	0.07812	0.1950	-0.1169	0.01050	0.0003*
	60 °C					
	Low energy vs. Medium energy	0.01222	0.03363	-0.02141	0.003362	0.0004*
	Low energy vs. High energy	0.01222	0.07364	-0.06142	0.008474	0.0060*
	Medium energy vs. High energy	0.03363	0.07364	-0.04002	0.008606	0.0126*
STR	**25 °C**					
	Low energy vs. Medium energy	0.01048	0.02828	-0.01780	0.004515	0.0015*
	Low energy vs. High energy	0.01048	0.1052	-0.09470	0.004241	0.0027*
	Medium energy vs. High energy	0.02828	0.1052	-0.07690	0.005187	0.0142*
	37 °C					
	Low energy vs. Medium energy	0.03248	0.06850	-0.03603	0.009364	0.0267*
	Low energy vs. High energy	0.03248	0.1937	-0.1612	0.01842	0.0015*
	Medium energy vs. High energy	0.06850	0.1937	-0.1252	0.01726	0.0067*
	44 °C					
	Low energy vs. Medium energy	0.04120	0.08368	-0.04248	0.006691	0.0006*
	Low energy vs. High energy	0.04120	0.2352	-0.1940	0.04161	0.0197*
	Medium energy vs. High energy	0.08368	0.2352	-0.1516	0.04166	0.0450*
	60 °C					
	Low energy vs. Medium energy	0.02035	0.05473	-0.03438	0.005197	0.0014*
	Low energy vs. High energy	0.02035	0.2091	-0.1888	0.02609	0.0098*
	Medium energy vs. High energy	0.05473	0.2091	-0.1544	0.02609	0.0177*

Table 1 (continued)

		Mean 1	Mean 2	Mean difference	SE difference	*p*-value
CYS	**25 °C**					
	Low energy vs. Medium energy	0.002120	0.01118	-0.009055	0.002191	0.0115*
	Low energy vs. High energy	0.002120	0.02462	-0.02250	0.004488	0.0074*
	Medium energy vs. High energy	0.01118	0.02462	-0.01345	0.004305	0.0613
	37 °C					
	Low energy vs. Medium energy	0.005500	0.03808	-0.03258	0.005174	0.0024*
	Low energy vs. High energy	0.005500	0.08368	-0.07818	0.005389	<0.0001*
	Medium energy vs. High energy	0.03808	0.08368	-0.04560	0.006839	0.0004*
	44 °C					
	Low energy vs. Medium energy	0.02030	0.02668	-0.006375	0.003877	0.3003
	Low energy vs. High energy	0.02030	0.08383	-0.06353	0.005313	0.0002*
	Medium energy vs. High energy	0.02668	0.08383	-0.05715	0.005455	0.0003*
	60 °C					
	Low energy vs. Medium energy	0.005600	0.05088	-0.04528	0.005660	0.0079*
	Low energy vs. High energy	0.005600	0.09612	-0.09052	0.009272	0.0013*
	Medium energy vs. High energy	0.05088	0.09612	-0.04525	0.01084	0.0123*
COD	**25 °C**					
	Low energy vs. Medium energy	0.02326	0.03486	-0.01160	0.01133	0.5849
	Low energy vs. High energy	0.02326	0.1658	-0.1425	0.02429	0.0273*
	Medium energy vs. High energy	0.03486	0.1658	-0.1309	0.02363	0.0392*
	37 °C					
	Low energy vs. Medium energy	0.01760	0.04486	-0.02726	0.01089	0.0908
	Low energy vs. High energy	0.01760	0.1709	-0.1533	0.01347	<0.0001*
	Medium energy vs. High energy	0.04486	0.1709	-0.1261	0.01494	0.0001*
	44 °C					
	Low energy vs. Medium energy	0.02464	0.08303	-0.05839	0.005469	0.0018*
	Low energy vs. High energy	0.02464	0.1449	-0.1203	0.01092	0.0028*
	Medium energy vs. High energy	0.08303	0.1449	-0.06190	0.01201	0.0120*
	60 °C					
	Low energy vs. Medium energy	0.05940	0.08267	-0.02327	0.01280	0.3118
	Low energy vs. High energy	0.05940	0.1375	-0.07806	0.009556	0.0003*
	Medium energy vs. High energy	0.08267	0.1375	-0.05479	0.01413	0.0403*
UA	**25 °C**					
	Low energy vs. Medium energy	0.009960	0.04704	-0.03708	0.01351	0.0925
	Low energy vs. High energy	0.009960	0.1545	-0.1445	0.01532	0.0009*
	Medium energy vs. High energy	0.04704	0.1545	-0.1074	0.01968	0.0016*
	37 °C					
	Low energy vs. Medium energy	0.003100	0.03626	-0.03316	0.01130	0.0834
	Low energy vs. High energy	0.003100	0.1400	-0.1369	0.005895	<0.0001*
	Medium energy vs. High energy	0.03626	0.1400	-0.1037	0.01243	0.0004*
	44 °C					
	Low energy vs. Medium energy	0.005380	0.04266	-0.03728	0.006735	0.0111*
	Low energy vs. High energy	0.005380	0.1663	-0.1609	0.01912	0.0024*
	Medium energy vs. High energy	0.04266	0.1663	-0.1236	0.02026	0.0041*
	60 °C					
	Low energy vs. Medium energy	0.01716	0.05243	-0.03527	0.01379	0.1394
	Low energy vs. High energy	0.01716	0.1036	-0.08644	0.02195	0.0323*
	Medium energy vs. High energy	0.05243	0.1036	-0.05118	0.02526	0.1826

is physiologically higher than what is clinically used. In the future, it would be of interest to optimize the laser dosimetry with a narrower temperature range for saline irrigation that is closer to clinical practice (25–37 °C). Also, while we sought to assess the impact of various fluid temperature settings on different laser pulse energies on uroliths with nearly pure chemical compositions; in the clinical world, there are often stones of mixed chemical compositions which challenge surgeons to fine-tune their laser settings throughout the procedure. This underscores the growing need for an AI

Table 2 A multivariate generalized linear model of stone ablation efficiency. β (beta weight) is a statistical metric used in multivariate generalized linear models that measures the relationship between a one-unit increase in the independent variables (i.e., temperature and energy) and the corresponding response in the dependent variable (i.e., the volume of the ablation cone). *p*-values marked with * have reached statistical significance

Parameter	b	95% Wald confidence interval	*p*-value
COM	0.022	0.009–0.036	0.001
CAP	0.014	0.001–0.027	0.042
STR	0.023	0.010–0.037	<0.001
CYS	-0.28	-0.042– -0.015	<0.001
COD	0.016	0.003–0.029	0.019
Energy (dJ)	0.009	0.009–0.010	<0.001
Temperature	0.001	0.001–0.001	<0.001

software capable of intraoperatively "reading" the stone's composition in real time, and then recommending or automatically selecting optimal laser settings during the entire laser lithotripsy procedure. Lastly, our study only concerns what may occur when the laser fiber is in direct perpendicular contact with the stone's surface. Again, during a clinical procedure, this distance and the angle at which the fiber addresses the stone's surface varies based on the irregularities in the stone's surface as most calculi do not have a planar surface.

Conclusion

Although statistically significant, the effect of increased fluid temperature on superpulse Thulium laser stone ablation is modest compared to that of minor increases in laser energy. Using a 37 °C irrigation fluid instead of the regular room temperature (25 °C) irrigation fluid would generate the same ablation cone by increasing the laser firing energy by only 0.18 J. Indeed, the benefit in ablation cone volume from continuous laser firing at temperatures as high as 44 °C is greatly outweighed by the risk of urothelial cytotoxicity, especially since the stone matrix acts as a "heat sink" As such, given the more sanguine postoperative clinical course when using irrigation at body temperature (i.e. 37 °C) and no discernible benefit if one increases the irrigant temperature higher, we currently set the irrigation at 37 °C for all of our ureteroscopic superpulse Thulium laser procedures.

Supplementary Information The online version contains supplementary material available at https://doi.org/10.1007/s10103-024-04253-2.

Author contributions R.V.C., J.L., T.M., and N.K. conceived the presented experiment. A.C., N.K., T.V., A.G., M.H., K.V., and Z.T. all contributed to the experiment and data collection. A.C., N.K., A.G., and Y.W. were involved in data analysis. A.C., N.K., T.V., A.G., R.V.C., and J.L. wrote the main manuscript text. A.C., N.K., and T.V. prepared all figures and tables. All authors reviewed the manuscript and agree with its contents.

Funding The authors declare they have no relevant financial or non-financial interests to disclose. The authors declare they have no sources of funding to disclose.

Data availability No datasets were generated or analysed during the current study.

Declarations

Competing interests The authors declare no competing interests.

References

1. Jones P, Beisland C, Ulvik Ø (2021) Current status of thulium fibre laser lithotripsy: an up-to-date review. BJU Int 128(5):531–538. https://doi.org/10.1111/bju.15551
2. Taratkin M, Laukhtina E, Singla N et al (2021) How lasers ablate stones: in vitro study of laser lithotripsy (Ho:YAG and Tm-Fiber lasers) in different environments. J Endourol 35(6):931–936. https://doi.org/10.1089/end.2019.0441
3. Taratkin M, Azilgareeva C, Cacciamani GE et al (2022) Thulium fiber laser in urology: physics made simple. Curr Opin Urol 32(2):166–172. https://doi.org/10.1097/mou.0000000000000967
4. Traxer O, Keller EX (2020) Thulium fiber laser: the new player for kidney stone treatment? A comparison with Holmium:YAG laser. World J Urol 38(8):1883–1894. https://doi.org/10.1007/s00345-019-02654-5
5. Chan KF, Pfefer TJ, Teichman JM et al (2001) A perspective on laser lithotripsy: the fragmentation processes. J Endourol 15(3):257–273. https://doi.org/10.1089/089277901750161737
6. Keller EX, de Coninck V, Audouin M et al (2019) Fragments and dust after holmium laser lithotripsy with or without Moses technology: how are they different? J Biophotonics 12(4):e201800227. https://doi.org/10.1002/jbio.201800227
7. Chan KF, Vassar GJ, Pfefer TJ et al (1999) Holmium:YAG laser lithotripsy: a dominant photothermal ablative mechanism with chemical decomposition of urinary calculi. Lasers Surg Med 25(1):22–37. https://doi.org/10.1002/(sici)1096-9101(1999)25:1%3C22::aid-lsm4%3E3.0.co;2-6
8. Vassar GJ, Chan KF, Teichman JM et al (1999) Holmium:YAG lithotripsy: photothermal mechanism. J Endourol 13(3):181–190. https://doi.org/10.1089/end.1999.13.181
9. Hardy LA, Irby PB, Fried NM (2018) Scanning electron microscopy of real and artificial kidney stones before and after Thulium fiber laser ablation in air and water. SPIE
10. Jansen ED, van Leeuwen TG, Motamedi M et al (1994) Temperature dependence of the absorption coefficient of water for midinfrared laser radiation. Lasers Surg Med 14(3):258–268. https://doi.org/10.1002/lsm.1900140308
11. King JB, Katta N, Teichman JMH et al (2021) Mechanisms of pulse modulated holmium:YAG lithotripsy. J Endourol 35(S3):S29–s36. https://doi.org/10.1089/end.2021.0742
12. Fujimoto JG, Brezinski ME, Tearney GJ et al (1995) Optical biopsy and imaging using optical coherence tomography. Nat Med 1(9):970–972. https://doi.org/10.1038/nm0995-970
13. Wang HW, Chen Y (2014) Clinical applications of optical coherence tomography in urology. Intravital 3(1):e28770. https://doi.org/10.4161/intv.28770
14. Dau JJ, Hall TL, Matzger AJ et al (2022) Laser heating of fluid with and without stone ablation: in vitro assessment. J Endourol 36(12):1607–1612. https://doi.org/10.1089/end.2022.0199

15. Aldoukhi AH, Hall TL, Ghani KR et al (2018) Caliceal fluid temperature during high-power holmium laser lithotripsy in an in vivo porcine model. J Endourol 32(8):724–729. https://doi.org/10.1089/end.2018.0395
16. Aldoukhi AH, Ghani KR, Hall TL et al (2017) Thermal response to high-power holmium laser lithotripsy. J Endourol 31(12):1308–1312. https://doi.org/10.1089/end.2017.0679
17. Maxwell AD, MacConaghy B, Harper JD et al (2019) Simulation of laser lithotripsy-induced heating in the urinary tract. J Endourol 33(2):113–119. https://doi.org/10.1089/end.2018.0485
18. Okhunov Z, Jiang P, Afyouni AS et al (2021) Caveat Emptor: the heat is ON- an in vivo evaluation of the thulium fiber laser and temperature changes in the porcine kidney during dusting and fragmentation modes. J Endourol 35(11):1716–1722. https://doi.org/10.1089/end.2021.0206
19. Noureldin YA, Farsari E, Ntasiotis P et al (2021) Effects of irrigation parameters and access sheath size on the intra-renal temperature during flexible ureteroscopy with a high-power laser. World J Urol 39(4):1257–1262. https://doi.org/10.1007/s00345-020-03287-9
20. Morgan KL, Jiang P, Peta A et al (2022) MP32-07: thermal effects of the super-pulse thulium fiber laser during ureteral stone laser lithotripsy: an in-vivo porcine study. J Urol 207(Supplement 5):e534. https://doi.org/10.1097/JU.0000000000002581.07
21. Pauchard F, Ventimiglia E, Corrales M et al (2022) A practical guide for intra-renal temperature and pressure management during rirs: what is the evidence telling us. J Clin Med 11(12). https://doi.org/10.3390/jcm11123429
22. Goldsmith L, Turney BW, Cleveland RO (2020) Effect of calculi on collecting system fluid temperature during holmium laser lithotripsy: in vitro model. Eur Urol Open Sci 19(e339). https://doi.org/10.1016/S2666-1683(20)32782-8
23. Marom R, Robinson J, Matzger AJ et al (2023) PD01-03: changes in stone core temperature: fragmentation vs. dusting. J Urol 209(Supplement 4):e63. https://doi.org/10.1097/JU.0000000000003218.03
24. Dau JJ, Hall TL, Maxwell AD et al (2021) Effect of chilled irrigation on caliceal fluid temperature and time to thermal injury threshold during laser lithotripsy: in vitro model. J Endourol 35(5):700–705. https://doi.org/10.1089/end.2020.0896
25. Hosseini SR, Mohseni MG, Aghamir SMK et al (2019) Effect of irrigation solution temperature on complication of percutaneous nephrolithotomy: a randomized clinical trial. Urol J 16(6):525–529. https://doi.org/10.22037/uj.v0i0.4399
26. Kati B, Buyukfirat E, Pelit ES et al (2018) Percutaneous nephrolithotomy with different temperature irrigation and effects on surgical complications and anesthesiology applications. J Endourol 32(11):1050–1053. https://doi.org/10.1089/end.2018.0581
27. Sea J, Jonat LM, Chew BH et al (2012) Optimal power settings for holmium:YAG lithotripsy. J Urol 187(3):914–919. https://doi.org/10.1016/j.juro.2011.10.147
28. Chan KF, Hammer DX, Choi B et al (2000) Free electron laser lithotripsy: threshold radiant exposures. J Endourol 14(2):161–167. https://doi.org/10.1089/end.2000.14.161
29. Robinson JW, Ghani KR, Roberts WW et al (2023) Near-infrared absorption coefficients in kidney stone minerals and their relation to crystal structure. J Phys Chem C 127(1):759–767. https://doi.org/10.1021/acs.jpcc.2c07475
30. Li C, Ban X, Zhang Y et al (2020) Rational design of disulfide bonds for enhancing the thermostability of the 1,4-α-glucan branching enzyme from geobacillus thermoglucosidans STB02. J Agric Food Chem 68(47):13791–13797. https://doi.org/10.1021/acs.jafc.0c04798